PHARMACEUTICAL BIOLOGY
2024, VOL. 62, NO. 1, 195–206
https://doi.org/10.1080/13880209.2024.2309891

Taylor & Francis
Taylor & Francis Group

RESEARCH ARTICLE

OPEN ACCESS Check for updates

Cephaeline promotes ferroptosis by targeting NRF2 to exert anti-lung cancer efficacy

Peng Chen[a], Qingxuan Ye[b], Shang Liang[b] and Linghui Zeng[a]

[a]Key Laboratory of Novel Targets and Drug Study for Neural Repair of Zhejiang Province, School of Medicine, Hangzhou City University, Hangzhou, PR China; [b]Department of Clinical Medicine, School of Medicine, Hangzhou City University, Hangzhou, PR China

ABSTRACT

Context: Cephaeline is a natural product isolated from ipecac (*Cephaelis ipecacuanha* [Brot.] A. Rich. [Rubiaceae]). It exhibits promising anti-lung cancer activity and ferroptosis induction may be a key mechanism for its anti-lung cancer effect.

Objectives: This study investigates the anti-lung cancer activity and mechanisms of cephaeline both *in vitro* and *in vivo*.

Materials and methods: H460 and A549 lung cancer cells were used. The cephaeline inhibition rate on lung cancer cells was detected *via* a Cell Counting Kit-8 assay after treatment with cephaeline for 24 h. Subsequently, the concentrations of 25, 50 and 100 nM were used for *in vitro* experiments. In addition, the antitumour effects of cephaeline (5, 10 mg/kg) *in vivo* were evaluated after 12 d of cephaeline treatment.

Results: Cephaeline showed significant inhibitory effects on lung cancer cells, and the IC_{50} of cephaeline on H460 and A549 at 24, 48 and 72 h were 88, 58 and 35 nM, respectively, for H460 cells and 89, 65 and 43 nM, respectively, for A549 cells. Meanwhile, we demonstrated that ferroptosis is the key mechanism of cephaeline against lung cancer. Finally, we found that cephaeline induced ferroptosis in lung cancer cells by targeting NRF2.

Discussion and conclusion: We demonstrated for the first time that cephaeline inhibits NRF2, leading to ferroptosis in lung cancer cells. These findings may contribute to the development of innovative therapeutics for lung cancer.

ARTICLE HISTORY
Received 15 May 2023
Revised 19 January 2024
Accepted 20 January 2024

KEYWORDS
Natural products; ipecac; GPX4; SLC7A11; TBHQ

Introduction

Lung cancer has the highest mortality rate of any malignant tumor worldwide (Sung et al. 2021). Histologically, lung cancer can be divided into non-small cell and small cell lung cancer (SCLC). Non-SCLC (NSCLC) patients account for approximately 85% of all lung cancer patients, with SCLC patients accounting for approximately 15% (Liu et al. 2015). The main treatments for lung cancer include surgery, radiotherapy and chemotherapy. However, in recent years, the emergence of treatments such as molecular targeted therapy and immunotherapy have diversified the options for treating lung cancer (Camidge et al. 2019). The induction of tumor cell apoptosis by chemotherapeutic drugs is one of the main methods for the clinical treatment of tumors. However, due to cancer cells becoming increasingly resistant to conventional programmed cell death treatments, research into other forms of cell death is necessary to develop new approaches for tumor therapy (Balaji et al. 2021).

Ferroptosis is a form of iron-dependent cell death, which occurs through excessive peroxidation of polyunsaturated fatty acids, and has characteristics that are different from apoptosis, necrosis and autophagy (Zhou et al. 2020; Dierge et al. 2021). The main features of ferroptosis include accumulation of iron ions, increased lipid peroxidation, increased lipid reactive oxygen species (ROS), smaller mitochondria and reduced cristae (Xie et al. 2016; Hirschhorn and Stockwell 2019). As a newly characterized form of cell death, there is an emerging focus on the induction of ferroptosis in the development of anticancer drugs.

Natural medicines have recently become an important source for the development of new antitumour drugs, mainly due to their unique roles in antitumour radiotherapy, and chemotherapy sensitization (Ashrafizadeh et al. 2020; Akter et al. 2021). Cephaeline is a natural product isolated from ipecac [*Cephaelis ipecacuanha* (Brot.) A.Rich. (Rubiaceae)]. Previous studies have shown that cephaeline confers a significant antitumour effect in mucoepidermoid carcinoma (MEC) and head and neck squamous cell carcinoma (HNSCC) (Qiang et al. 2022; Silva et al. 2022). However, whether cephaeline has a significant antitumour effect on lung cancer remains unclear. Our aim was to characterize the anti-lung cancer effects and mechanisms of cephaeline in the hopes of opening up a novel pathway for the development of lung cancer therapeutics.

CONTACT Peng Chen chenp@zucc.edu.cn Key Laboratory of Novel Targets and Drug Study for Neural Repair of Zhejiang Province, School of Medicine, Hangzhou City University, 50 Huzhou Rd, Hangzhou, Zhejiang, 310015, PR China

Materials and methods

Reagents and antibodies

Purified cephaeline (>98%) (cas: 483-17-0) was purchased from Chengdu Biopurify Phytochemicals Ltd. (Chengdu, China). DMSO (cat #D8371) was purchased from MP Biomedicals, LLC. (Santa Ana, CA). The following materials were also purchased: Cell Counting Kit-8 (CCK-8) (Dojindo, cat#CK04, Kumamoto, Japan). Reactive Oxygen Species Assay Kit (Beyotime, cat#S0033M, Shanghai, China). FerroOrange (Dojindo, cat#F374, Kumamoto, Japan). DAPI Staining Solution (Beyotime, cat#C1006, Shanghai, China). Mito-Tracker Red CMXRos fluorescent probe (Beyotime, cat#C1052, Shanghai, China). C11 BODIPY 581/591 (GLPBIO, cat#GC40165, Montclair, CA, USA). TRIzol reagent (Invitrogen, cat#15596026, Carlsbad, CA). GSH assay kit (Nanjing Jiancheng, cat#A006-2-1, Nanjing, China). MDA assay kit (Nanjing Jiancheng, cat#A003-1-2, Nanjing, China). RIPA Lysis Buffer (Beyotime, cat# P0013, Shanghai, China). BCA Protein Assay Kit (Beyotime, cat# P0012S, Shanghai, China). BeyoECL Plus (Beyotime, cat#P0018M, Shanghai, China). cDNA Synthesis SuperMix (Yeasen, cat#11141ES60, Shanghai, China). Real-time quantitative PCR SYBR Green Master Mix (Yeasen, cat#11201ES03, Shanghai, China). Necrostatin-1 (MCE, cat#HY-15760, Monmouth Junction, NJ, USA). Chloroquine (MCE, cat#HY-17589A, Monmouth Junction, NJ). Liproxstatin-1 (MCE, cat#HY-12726, Monmouth Junction, NJ). Z-VAD-FMK (MCE, cat#HY-16658B, Monmouth Junction, NJ). Ferrostatin-1 (MCE, cat#HY-100579, Monmouth Junction, NJ). Goat Serum (Solarbio, cat#SL038, Beijing, China). GPX4 (Abclonal, cat#A1933, Wuhan, China). SLC7A11/xCT (Abclonal, cat#A2413, Wuhan, China). Transferrin (Abclonal, cat#A19130, Wuhan, China). SLC40A1 (Abclonal, cat#A14885, Wuhan, China). NRF2 (Abclonal, cat# A3577, Wuhan, China).

Cell culture

H460 and A549 human lung cancer cell lines were purchased from American Type Culture Collection (ATCC) and cultured in Roswell Park Memorial Institute (RPMI)-1640 medium (Gibco, cat# 31800, Carlsbad, CA) supplemented with 10% foetal bovine serum (FBS), 100 U/mL penicillin, and 1% streptomycin. Cells were incubated in a humidified atmosphere of 5% CO_2 at 37 °C.

Cell viability assay

The inhibitory effects of cephaeline on lung cancer cells were detected by CCK-8. The CCK-8 kit is a rapid, highly sensitive, non-radioactive colorimetric detection kit based on WST-8, which is widely used in cell proliferation and cytotoxicity assays. A549 and H460 cell lines were seeded in 96-well plates (Corning plate, cat#430196, Corning, NY) with a density of 5×10^3 per well (100 µL) before being placed in an incubator for pre-incubation for 24 h. The cells were then treated with different concentrations of cephaeline (5, 15, 25, 50, 100, 200 and 400 nM) at 24, 48 and 72 h, respectively. Finally, 10 µL of CCK-8 solution was added to each well, before incubation of the plate in an incubator for 1–4 h. The absorbance was measured at 450 nm with a microplate reader. Calculate IC_{50} value using GraphPad Prism. First, a datasheet was created to correlate the logarithm of cephaeline concentrations (5, 15, 25, 50, 100, 200 and 400 nM) with the percentage of response. Subsequently, IC_{50} values and standard errors were determined using nonlinear regression curve fitting.

Measurement of Fe^{2+}

H460 and A549 cells were seeded in 6-well plates (Corning plate, cat#430196, Corning, NY) at a density of 6×10^5/well and incubated overnight at 37 °C in a 5% CO_2 incubator. Then cells were treated with cephaeline (25, 50 and 100 nM) for 24 h and the supernatant was discarded and the cells were washed three times with HBSS or serum-free medium. FerroOrange working solution was added at a concentration of 1 µmol/L and incubated at 37 °C in a 5% CO_2 incubator for 30 min. Subsequently, the cells were observed under a fluorescence microscope.

Measurement of ROS levels

H460 and A549 cell lines were seeded in 6-well plates at a density of 6×10^5/well. The cells were incubated with or without cephaeline (25, 50 and 100 nM) treatment for 24 h, after which the culture supernatants were removed and 10 µmol/L DCFH-DA was added and cells were incubated in a 37 °C cell incubator for 20 min. Cells were washed three times with serum-free cell culture medium and detected by fluorescence microscopy or flow cytometry.

Measurement of MDA

Malondialdehyde (MDA) levels were measured using a Lipid Peroxidation MDA Assay Kit, according to the manufacturer's instructions. H460 and A549 cell lines were seeded in 6-well plates at a density of 6×10^5/well and treated with cephaeline (25, 50 and 100 nM) for 24 h. The cells were then collected and lysed. The protein concentration of the samples was then measured. Subsequently, 100 µL of H460 cell lysates from the different treatment groups (Control, 25, 50 and 100 nM) with protein concentrations of 2, 2, 1 and 1 mg/mL, and 100 µL of A549 cell lysates from different treatment groups (Control, 25, 50 and 100 nM) with protein concentrations of 2, 2, 1 and 1 mg/mL were treated with the MDA assay solution (1000 µL) at 100 °C for 40 min, and centrifuged at 4000 *g* for 10 min. Finally, 250 µL of the supernatant was added to a 96-well plate and the absorbance measured at 530 nm. The MDA level was calculated as nmol/mg protein.

Measurement of GSH

The glutathione (GSH) contents were measured by a GSH assay kit according to the manufacturer's instructions. H460 and A549 cell lines were seeded in 6-well plates at a density of 6×10^5/well. Cells were then collected and lysed after 24 h of treatment with cephaeline and protein concentration of samples were measured. Then the samples were centrifuged at 3500 *g* for 10 min at 4 °C. The supernatant was treated with Ellman's reagent (DTNB) in combination with GSH to generate a yellow compound. Finally, the absorbance was measured at 405 nm using a microplate reader. The GSH level was calculated as µmol/g protein.

Real-time PCR

H460 and A549 cells were seeded in six well plates at a density of 6×10^5/well and cultured in a cell incubator for 24 h. After cephaeline treatment for 24 h, a total of 3 µg RNA was extracted

using TRIzol reagent. cDNA Synthesis SuperMix was used for reverse transcription experiments. The SYBR-Green-based detection kit was used for real-time quantitative PCR on the real-time PCR detection System (Bio-rad CFX96™, Hercules, CA), according to the manufacturer's instructions. The results were analysed by $2^{-\Delta\Delta Cq}$ method (Huang et al. 2019). The primers used are listed in Table 1.

Western blot

H460 and A549 cell lines were seeded in 6-well plates at a density of 6×10^5/well. Cells with or without cephaeline treated for 24 h, the cell pellet collected was added to a corresponding volume of lysis buffer (20 mM Tris (pH7.5), 150 mM NaCl, 1% Triton X-100, sodium pyrophosphate, β-glycerophosphate, EDTA, Na3VO4, leupeptin) purchased from Beyotime, lysed for 20 min, and the centrifuge tube was placed on a vortex shaker for 10 s every 5 min. The sample was placed in a pre-cooled high-speed refrigerated centrifuge at 12,000 *g* for 15 min. The supernatant was aspirated for protein concentration determination by BCA kit. Loading buffer was then added and the sample was heated at 95 °C for denaturation for 10 min and stored at −20 °C after the liquid was completely cooled. The 10–12% sodium dodecyl sulphate-polyacrylamide gel electrophoresis (SDS-PAGE) was used to separate proteins, and then the proteins were transferred into polyvinylidene fluoride (PVDF) membranes, followed by blocking using 5% skimmed milk at the room temperature (20–25 °C) for 1 h and incubation with the primary antibody (1:1000) overnight at 4 °C. After washing, the secondary antibody (1:1000) was added before incubation at room temperature for 1 h. After washing again, the chemiluminescence detection kit BeyoECL Plus was used for detection of the membrane.

In vivo *tumor model*

All *in vivo* animal experimental procedures were approved by the Institutional Animal Care and Use Committee at Zhejiang Academy of Medical Sciences (approval no ZJCLA-IACUC-20010409). Five-week-old female BALB/c-nu mice were purchased from the Zhejiang Academy of Medical Sciences. After a period of adaptive feeding, the lung cancer H460 cell line (1×10^6 cells in 0.1 mL PBS) was injected into the right dorsal flank of each mouse to establish the subcutaneous tumor model. After the model was successfully constructed, 24 mice were randomly divided into four groups; the control group (solvent), erastin group (20 mg/kg), and the cephaeline treatment group (5, 10 mg/kg). After 12 d of intraperitoneal injection, the mice were sacrificed by CO_2 asphyxiation, and tumor tissues were collected for subsequent evaluation.

Table 1. Primer sequences used.

Primers		
GPX4	Forward primer	CGCTGTGGAAGTGGATGAAG
	Reverse primer	TTGTCGATGAGGAACTGTGG
SLC7A11	Forward primer	TTTTGTACGAGTCTGGGTGG
	Reverse primer	CGCAAGTTCAGGGATTTCAC
SLC40A1	Forward primer	GGGTGGACAAGAATGCTAGAC
	Reverse primer	ATGGTACATGGTCAGAAGCTC
Transferrin	Forward primer	TGAGCCACGTAAACCTCTTG
	Reverse primer	AGTATTGGTTAAGGGTGGAGC
β-Actin	Forward primer	CTCCATCCTGGCCTCGCTGT
	Reverse primer	GCTGTCACCTTCACCGTTCC

Statistical analysis

Data were expressed as mean ± SD. The results were analysed with a one-way ANOVA or Student's *t*-test. All statistical analyses were performed using GraphPad Prism 7.0c (GraphPad Software, La Jolla, CA). Values of $^*p < 0.05$, $^{**}p < 0.01$ were considered statistically significant.

Results

Cephaeline induces lung cancer cell death in vitro

Cell Counting Kit-8 (referred to as CCK-8 kit) was used to assay the antitumour effects of cephaeline *in vitro*. We found that cephaeline with different concentrations (5, 15, 25, 50, 100, 200 and 400 nM) conferred a significant inhibitory effect on lung cancer cells at different time of 24, 48 and 72 h. Based on the inhibition of different concentrations of cephaeline on H460 and A549 lung cancer cells, we calculated that the IC_{50} of cephaeline on lung cancer cells H460 and A549 at 24, 48 and 72 h were 88, 58 and 35 nM, respectively, for H460 cells and 89, 65 and 43 nM, respectively, for A549 cells (Figure 1(A,B)).

Cephaeline induces ferroptosis in lung cancer cells by targeting NRF2

Detection of ROS levels using the fluorescent probe DCFH-DA showed that cephaeline can promote the upregulation of ROS levels (Figure 2(A)). In addition, Mito Tracker Red CMXRos, a mitochondrial membrane potential fluorescent probe, was used to detect the effect of cephaeline on the changes of mitochondrial membrane potential in lung cancer cells. We observed that compared with the control group, mitochondrial membrane potentials were decreased after treatment of the cells with cephaeline for 24 h. Moreover, the mitochondrial ultrastructure was observed using a transmission electron microscope, we found that compared with the control group, the mitochondrial cristae vanished and the mitochondrial volume decreased after cephaeline treatment (Figure 2(B,C)). Subsequently, we found that apoptosis, necroptosis and autophagy inhibitors had no obvious reversal effects on cephaeline-induced cell death (Figure 3(A)). However, the inhibitory effects of cephaeline on lung cancer cells were significantly reversed after administration of the ferroptosis inhibitors (liproxstatin-1 [Lip-1], ferrostatin-1 [Fer-1] and deferoxamine [DFO]), suggesting that cephaeline may induce ferroptosis in lung cancer cells (Figure 3(B)). Detection of iron levels using a FerroOrange fluorescent probe showed that iron levels were markedly elevated in the cephaeline-treated group (Figure 3(C)).

In addition, as iron ions can cause severe lipid peroxidation in cells, which leads to iron-dependent cell death, lipid peroxidation was measured using a C11 BODIPY 581/591 fluorescent ratio-probe. The levels of LPO and MDA, as indicators of lipid peroxidation, were also detected. The results showed that cephaeline significantly induced lipid peroxidation in lung cancer cells, accompanied by the release of large amounts of LDH, an important hallmark of cell death closely associated with cell membrane damage (Figure 4(A–E)).

Moreover, we found that the content of the key antioxidant GSH in cells was significantly reduced with aggravation of cephaeline-induced lipid peroxidation (Figure 4(F)). Therefore, to verify that iron-induced lipid peroxidation was the key cause of cephaeline-induced cell death, the antioxidants NAC and GSH

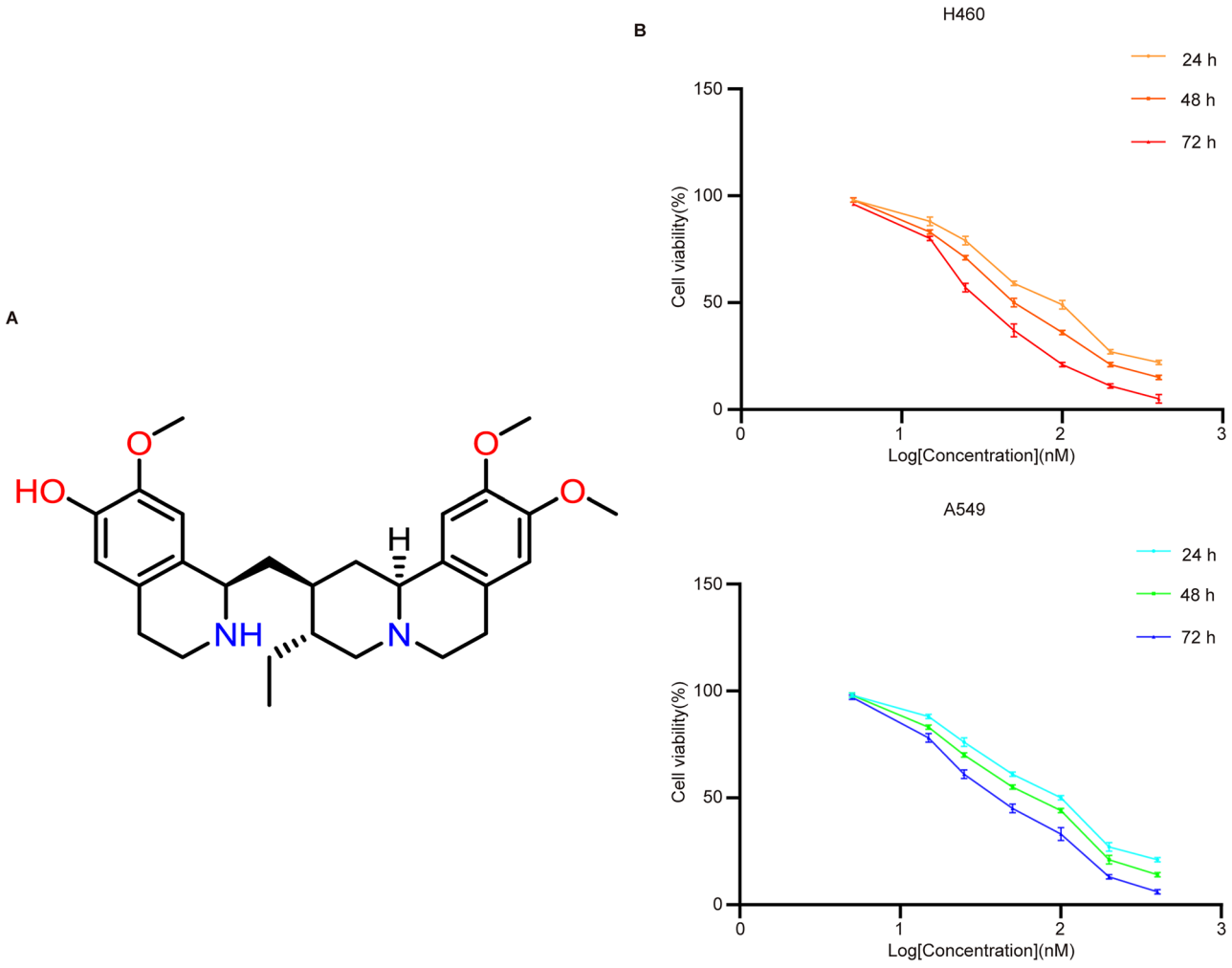

Figure 1. Cephaeline induces lung cancer cell death *in vitro*. (A) The structure of cephaeline. (B) CCK-8 was used to detect the effect of different concentrations of cephaeline on the cell viability of lung cancer cell line H460 and A549 at different time points (24, 48 and 72 h).

were co-administrated with cephaeline to investigate whether antioxidants could reverse cephaeline-induced cell death. The results showed that cell viability was significantly upregulated by administration of the antioxidants with cephaeline compared with the group treated only with cephaeline (Figure 4(G,H)). Subsequently, the expression of ferroptosis-related genes was measured by real-time PCR, showing that cephaeline significantly downregulated the key antioxidant genes GPX4 and SLC7A11. However, cephaeline also significantly upregulated transferrin, a regulatory gene that promotes iron influx, and significantly downregulated SLC40A1, a regulatory gene that controls iron efflux (Figure 5(A–D)). In addition, investigation of the corresponding protein levels using western blotting showed that the protein expression was consistent with the gene expression (Figure 5(E–I)). Finally, to determine the specific mechanism of ferroptosis induction by cephaeline, the expression of the key antioxidant regulatory protein NRF2 was measured in cells, finding that cephaeline significantly inhibited the expression of NRF2 (Figure 5(J–L)).

Inhibitory effects of cephaeline on lung cancer cells are alleviated by an NRF2 agonist

To further confirm that cephaeline plays a role in inducing ferroptosis by targeting NRF2 in lung cancer cells. The NRF2 agonist *tert*-butylhydroquinone (TBHQ) was pre-treated with lung cancer cells, and we found that the death of lung cancer cells induced by cephaeline was significantly alleviated (Figure 6(A)). Meanwhile, lipid ROS levels and lipid peroxidation were detected in the cephaeline treatment groups with or without TBHQ pretreatment. It was found that TBHQ significantly reversed the increases in both lipid ROS and lipid peroxidation induced by cephaeline (Figure 6(B,C)). Moreover, GSH levels were elevated in the cephaeline treatment group when pretreated with TBHQ (Figure 6(D)). Furthermore, the significantly elevated levels of LDH that were released by the cells treated with cephaeline were significantly reversed by TBHQ (Figure 6(E)). Finally, the expression of downstream ferroptosis-related target proteins GPX4 and SLC7A11 regulated by NRF2 were detected, and it was found that TBHQ could significantly reverse the expression of GPX4 and SLC7A11 (Figure 6(F,G)). Therefore, based on the above studies, it was fully demonstrated that cephaeline can induce ferroptosis in lung cancer cells by targeting NRF2

Cephaeline has inhibitory effects on lung cancer cells in vivo

To investigate the antitumour effects of cephaeline *in vivo*, a subcutaneous tumor xenograft model was constructed. After

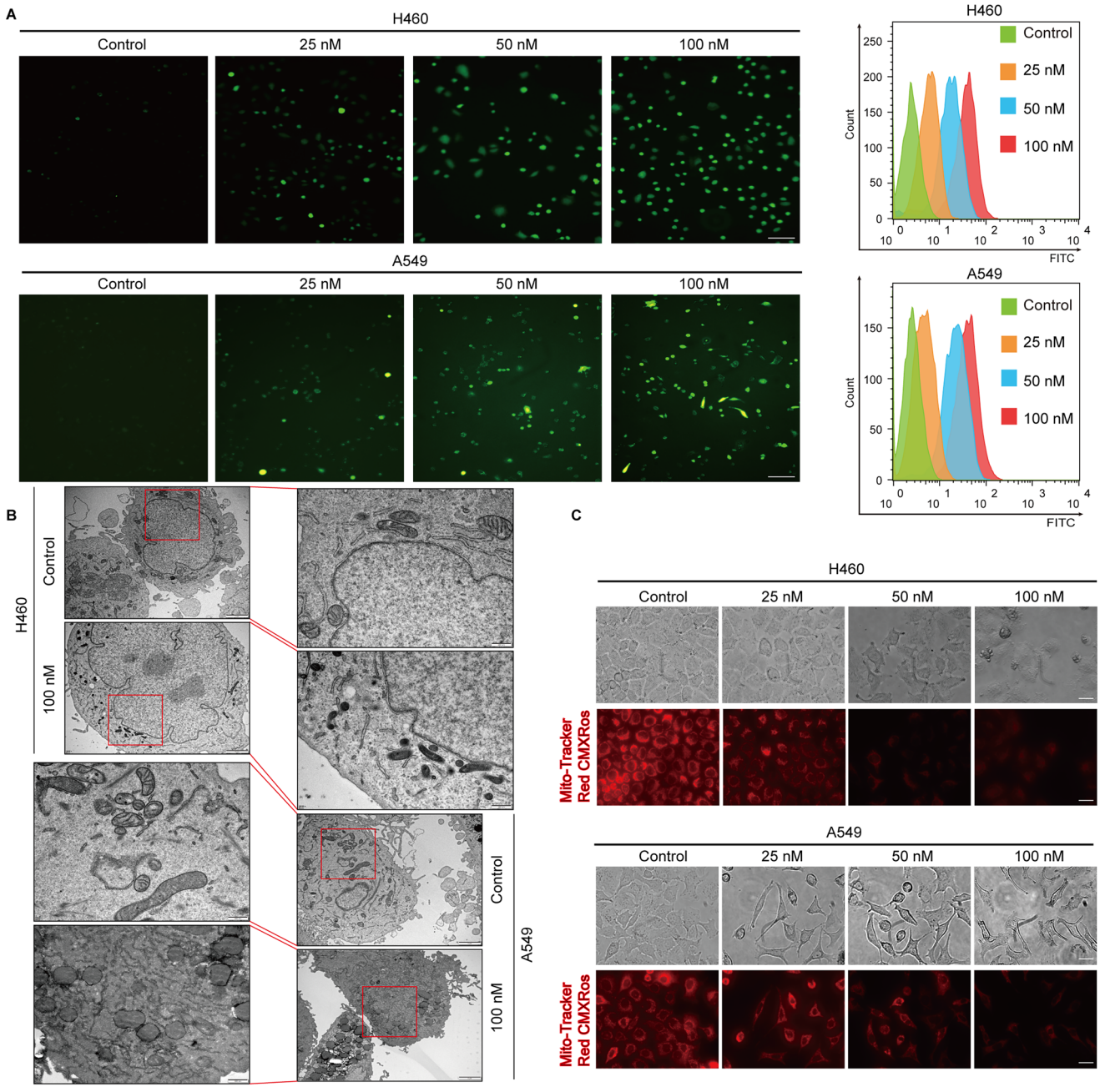

Figure 2. Cephaeline induces upregulation of ROS levels and mitochondrial damage. (A) The ROS level was determined by DCFH-DA probe after treatment with cephaeline for 24 h. Scale bars, 50 μm. (B) The mitochondrial morphological changes were detected by transmission electron microscopy after treatment with cephaeline for 24 h. Scale bars, 500 nm. (C) The changes in mitochondrial membrane potential were detected by Mito-Tracker Red CMXRos probe after treatment with cephaeline for 24 h. Scale bars, 20 μm.

12 d of drug treatment, it was found that 5 and 10 mg/kg cephaeline conferred significant antitumour effects *in vivo* compared with the control group. Meanwhile, the ED_{50} was 3 mg/kg and minimum effective concentration (MEC) was 2.5 mg/kg measured in subcutaneous tumor xenograft model. However, 10 mg/kg cephaeline had the same anti-lung cancer effect *in vivo* as the ferroptosis inducer erastin (Figure 7(A–D)). Meanwhile, it was also found that there were no significant differences in body weight between the mice in the cephaeline, erastin and the control groups (Figure 7(E)). Moreover, to verify that cephaeline plays an anti-lung cancer role by inducing ferroptosis *in vivo*, we detected the key proteins of ferroptosis in different groups of tumor tissues by western blot, and the results were consistent with the *in vitro* findings (Figures 7(F) and 8).

Discussion

Lung cancer is one of the most common malignant tumors worldwide. Moreover, the high morbidity and mortality of lung cancer are a serious threat to people's lives and health (Gao et al. 2020). However, due to the emergence of complicating issues such as apoptosis evasion and chemotherapy resistance in clinical practice, the important role of other non-apoptotic programmed cell death in tumor treatment is receiving increasing attention (Yang Y et al.

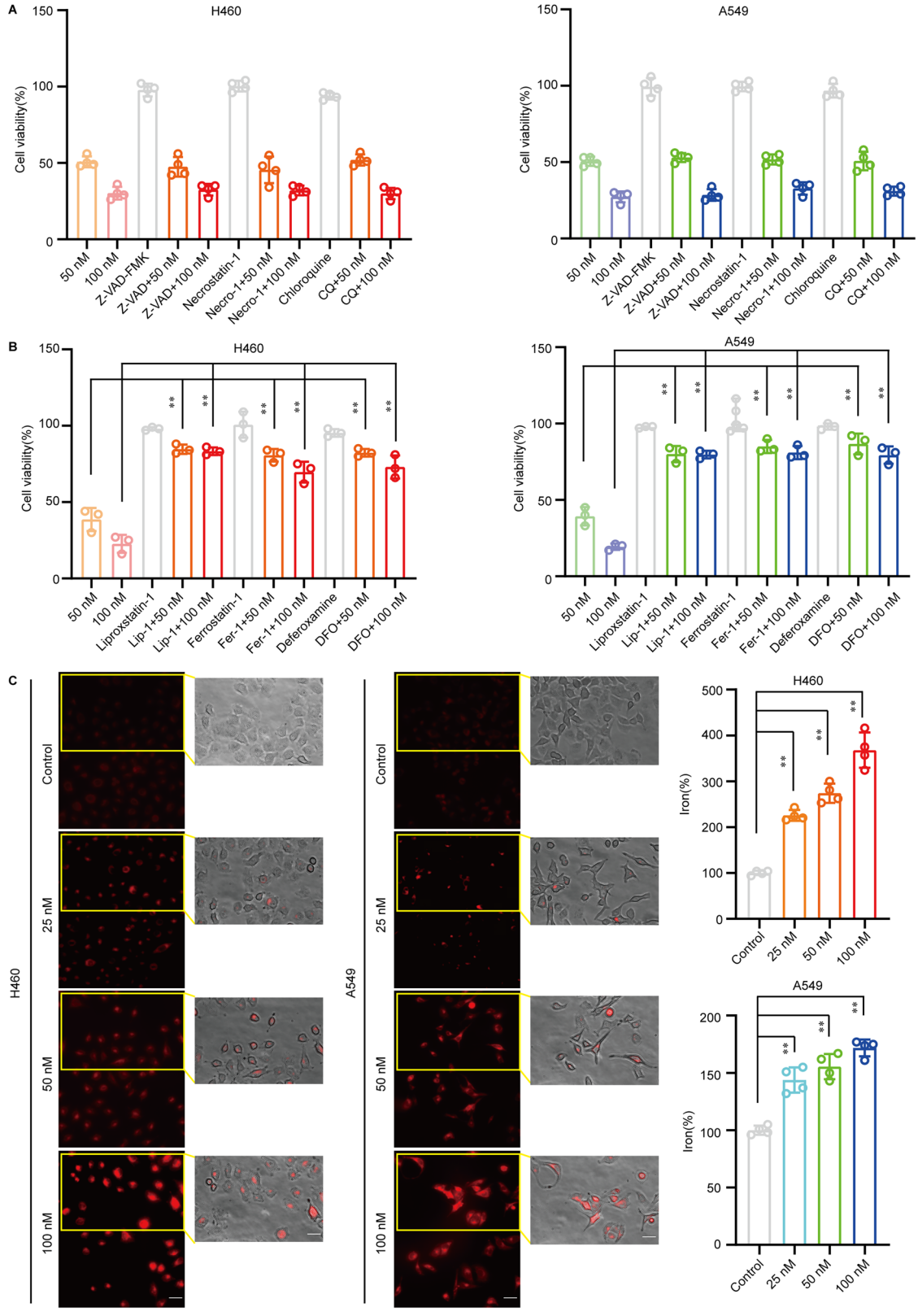

Figure 3. Cephaeline induces ferroptosis in lung cancer cells. (A) The reversal effect of apoptosis inhibitors (Z-VAD-FMK, 50 μM), necroptosis inhibitors (Necrostatin-1, 200 nM) and autophagy inhibitors (Chloroquine, 25 μM) on cephaeline induced lung cancer cell death. Mean ± SD, $^{**}p < 0.01$ *vs.* the cephaeline treatment group, $n = 4$. (B) The reversal effect of ferroptosis inhibitors [liproxstatin-1 (100 nM)/Ferrostatin-1 (2 μM)/Deferoxamine (100 μM)] on cephaeline induced lung cancer cell death, $n = 3$. Mean ± SD, $^{**}p < 0.01$ *vs.* the cephaeline treatment group. (C) The iron level was detected by FerroOrange fluorescent probe after treatment with cephaeline for 24 h. Scale bars, 10 μm. Mean ± SD, $^{**}p < 0.01$ *vs*. the control group.

2021). Ferroptosis is a new type of non-apoptotic programmed cell death discovered in recent years, which may become a new strategy for tumor treatment. Research has shown a significant association between ferroptosis and the survival and prognosis of tumor patients (Liang J et al. 2020; Wang D et al. 2021; Zhu G et al. 2021). For example, GPX4 is a key regulator of ferroptosis, and studies have

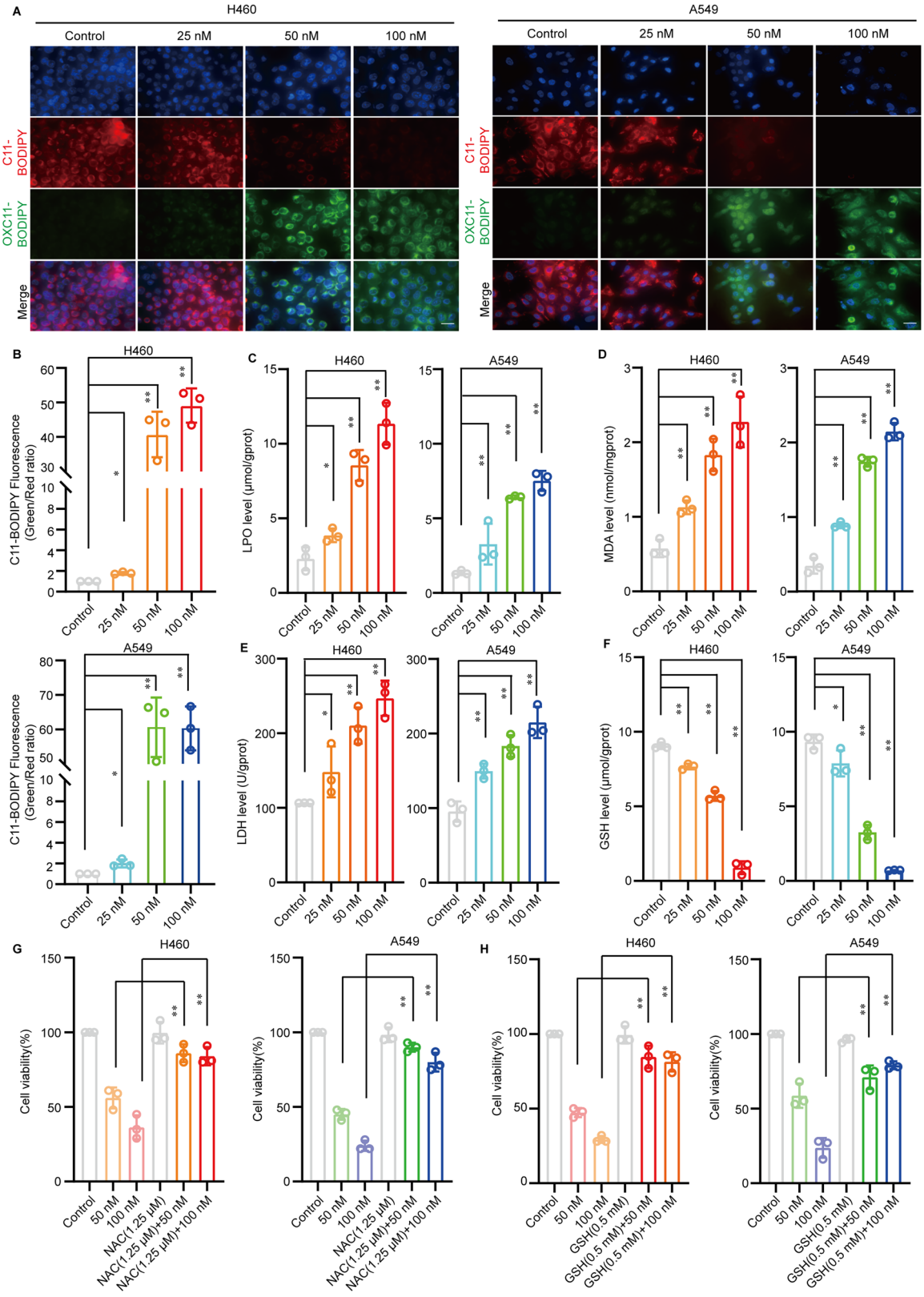

Figure 4. Cephaeline induces lipid peroxidation in lung cancer cells. (A and B) The lipid peroxidation was measured by C11 BODIPY 581/591 fluorescent ratio-probe in H460 and A549 cells after treatment with cephaeline for 24 h, Mean ± SD, $*p < 0.05$, $**p < 0.01$ *vs.* the control group. Scale bars, 10 μm. (C and D) The indicator of lipid peroxidation LPO, MDA was detected in H460 and A549 cells after treatment with cephaeline for 24 h, $n = 3$. Mean ± SD, $**p < 0.01$ *vs.* the control group. (E) Effect of cephaeline on LDH release was detected after treatment with cephaeline for 24 h, $n = 3$. Mean ± SD, $*p < 0.05$, $**p < 0.01$ *vs.* the control group. (F) The key antioxidant GSH was detected after treatment with cephaeline for 24 h, $n = 3$. Mean ± SD, $*p < 0.05$, $**p < 0.01$ *vs.* the control group. (G and H) The reversal effect of antioxidants NAC and GSH on cephaeline-induced cell death, $n = 3$. Mean ± SD, $**p < 0.01$ *vs.* the control group.

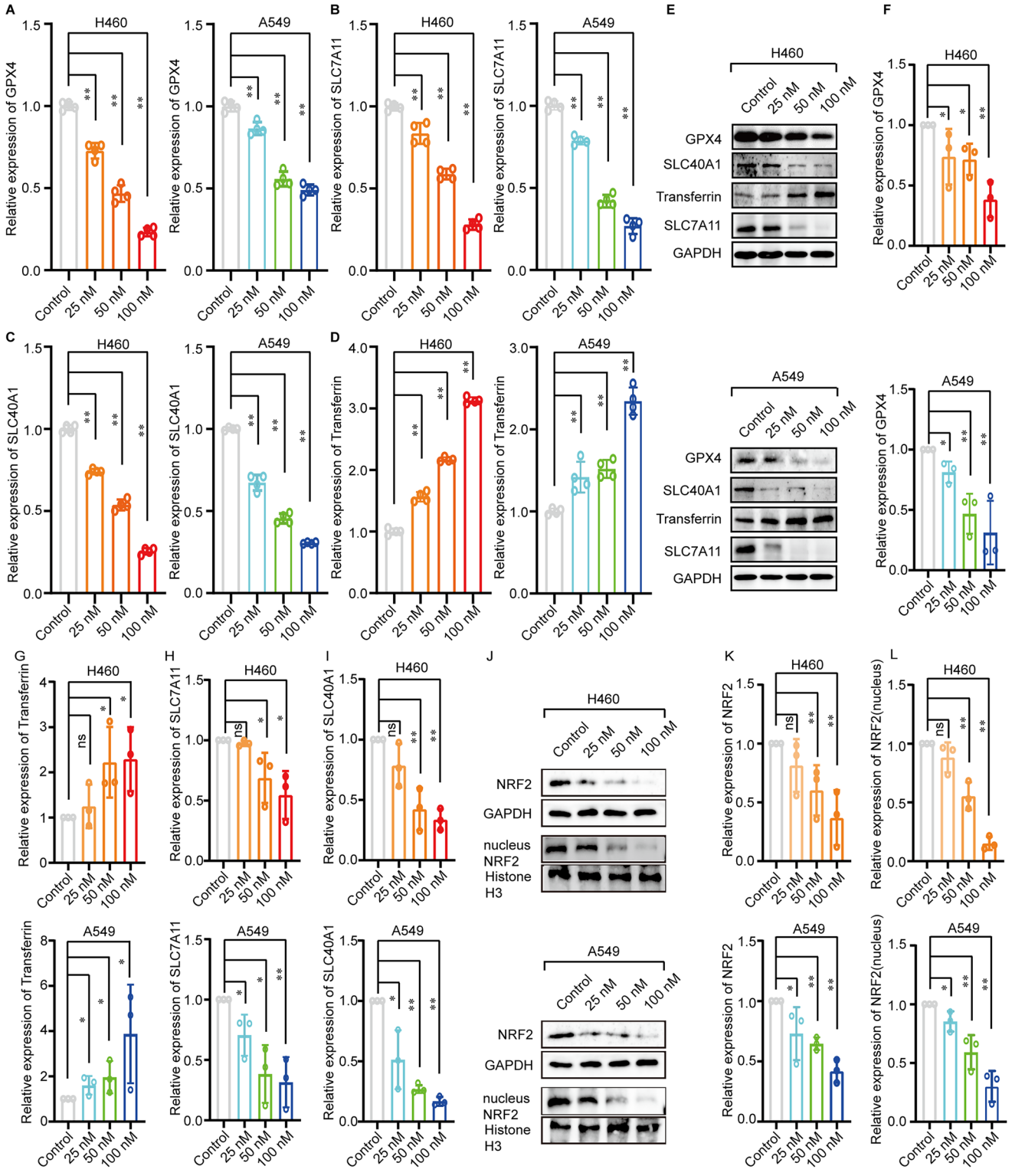

Figure 5. Effect of cephaeline on ferroptosis related genes and proteins in lung cancer cells. (A–D) The ferroptosis-related genes GPX4, SLC7A11, SLC40A1 and Transferrin were detected by RT-PCR in H460 and A549 cells after treatment with cephaeline for 24 h, $n = 3$. Mean ± SD, $^{**}p < 0.01$ *vs.* the control group. (E–I) The ferroptosis-related proteins GPX4, SLC7A11, SLC40A1 and Transferrin were detected by western blot in H460 and A549 cells after treatment with cephaeline for 24 h, repeated three times, Mean ± SD, $^{*}p < 0.05$, $^{**}p < 0.01$ *vs.* the control group. (J–L) The key antioxidant regulatory protein NRF2 was detected by western blot in H460 and A549 cells after treatment with cephaeline for 24 h, $n = 3$, Mean ± SD, $^{*}p < 0.05$, $^{**}p < 0.01$ *vs.* the control group.

shown that higher GPX4 expression is associated with better distant metastasis free survival rate of breast cancer (Sha R et al. 2021). Moreover, research has found that overexpression of SLC7A11, another key regulator of ferroptosis, is predictive of poor prognosis in lung cancer patients (Qian L et al. 2022). Therefore, screening drugs that can induce ferroptosis in tumor cells is expected to become a new strategy for the clinical management of tumors. There are currently few studies on the antitumour effects of cephaeline, particularly its anti-lung cancer effects. Accordingly, this study investigated the anti-lung cancer effect of cephaeline, and we found that cephaeline has significant inhibitory effects on lung cancer cells. Furthermore, we also found that the antitumour effects of

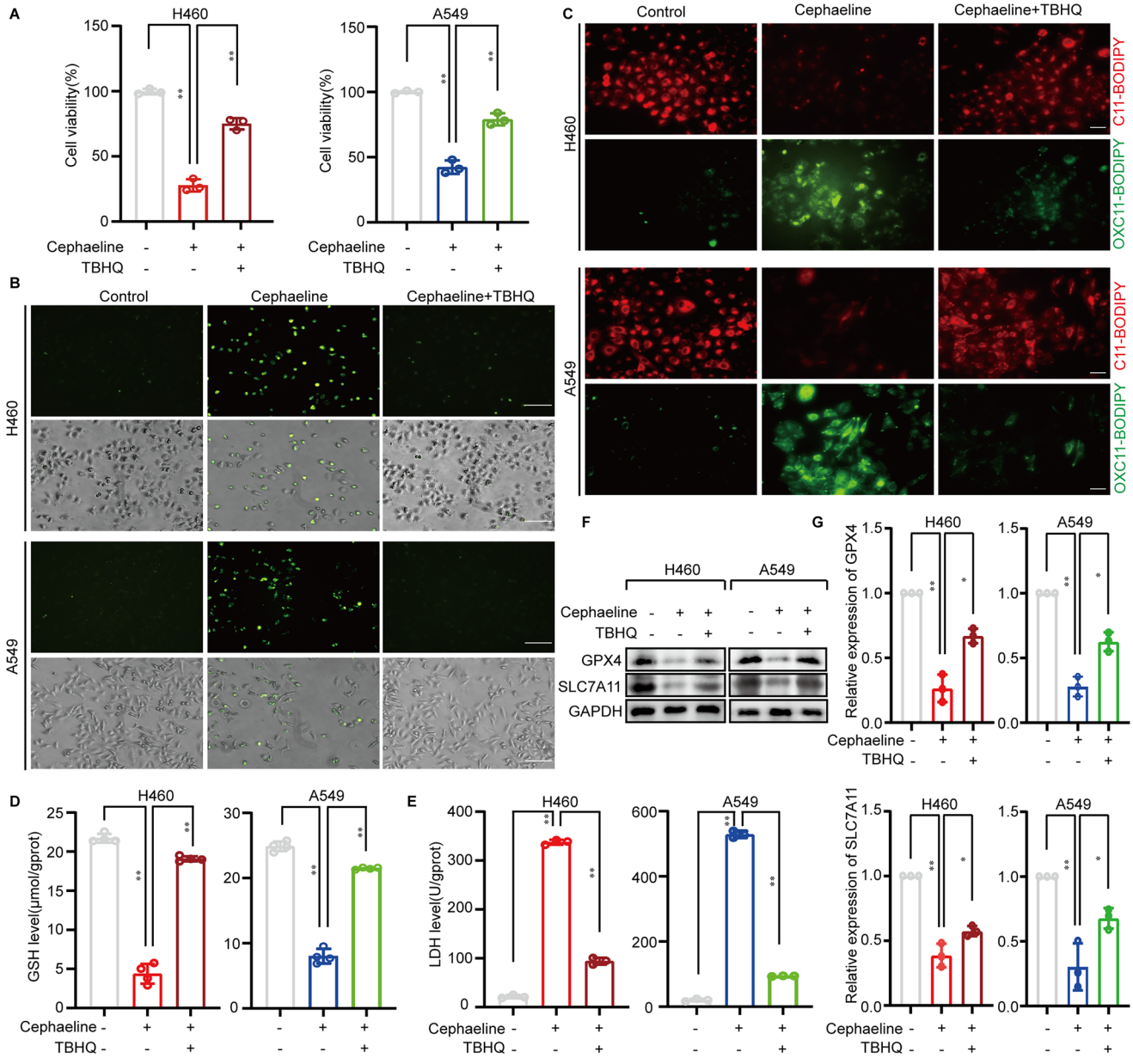

Figure 6. Inhibitory effects of cephaeline on lung cancer cells are alleviated by an NRF2 agonist. (A) The CCK-8 was used to detect the reversal effect of TBHQ (10 μM) on cephaeline (100 nM) induced lung cancer cell death, $n = 3$, Mean ± SD, $^{**}p < 0.01$ *vs.* the control group. (B) Using DCFH-DA probe to detect ROS level in control group, cephaeline treatment group and cephaeline combined TBHQ group. Scale bars, 50 μm. (C) The lipid peroxidation was measured by C11 BODIPY 581/591 fluorescent ratio-probe in control group, cephaeline treatment group and cephaeline combined TBHQ group. Scale bars, 20 μm. (D and E) Effect of cephaeline on LDH release and the key antioxidant GSH was detected in control group, cephaeline treatment group and cephaeline combined TBHQ group, $n = 3$. Mean ± SD, $^{**}p < 0.01$ *vs.* the control group. (F and G) The ferroptosis-related proteins GPX4, SLC7A11 were detected by western blot in control group, cephaeline treatment group and cephaeline combined TBHQ group, repeated three times, Mean ± SD, $^{*}p < 0.05$, $^{**}p < 0.01$ *vs.* the control group.

cephaeline were not reversed when lung cancer cells were pretreated with apoptosis, necrosis and autophagy inhibitors. However, the antitumour effects of cephaeline were reversed after pretreatment with ferroptosis inhibitors, indicating that ferroptosis induction may be the key antitumour mechanism of cephaeline.

Intracellular iron upregulation is the key feature of ferroptosis (Dixon et al. 2012). We found that cephaeline significantly promoted upregulation of intracellular iron upregulation. Moreover, structural changes in the mitochondria are another key sign of ferroptosis, and mitochondria mainly affect the occurrence and development of ferroptosis by regulating lipid metabolism, iron metabolism and glutamine decomposition (Xie et al. 2016; Gao et al. 2019; Wang et al. 2020; Mao et al. 2021). The results showed that cephaeline induced mitochondrial damage and decreased the mitochondrial membrane potential in lung cancer cells. In addition, due to the iron-dependent increase of lipid ROS can induce lipid peroxidation, which eventually leads to ferroptosis of lung cancer cells (Henning et al. 2022). Therefore, we found that the tumor suppressive effects of cephaeline were significantly reversed after pretreatment with antioxidants.

Subsequently, ferroptosis-related genes were detected by real-time PCR, we found that GPX4, SLC7A11 and SLC40A1 were downregulated, while the expression of transferrin gene was upregulated, and the expression changes of these genes were consistent with the corresponding protein expression. The downregulation of GPX4 and SLC7A11 led to the depletion of intracellular GSH and inhibition of the antioxidant system. However, when the expression of transferrin was upregulated, the downregulation of SLC40A1 promoted intracellular iron level upregulation, which was accompanied by lipid

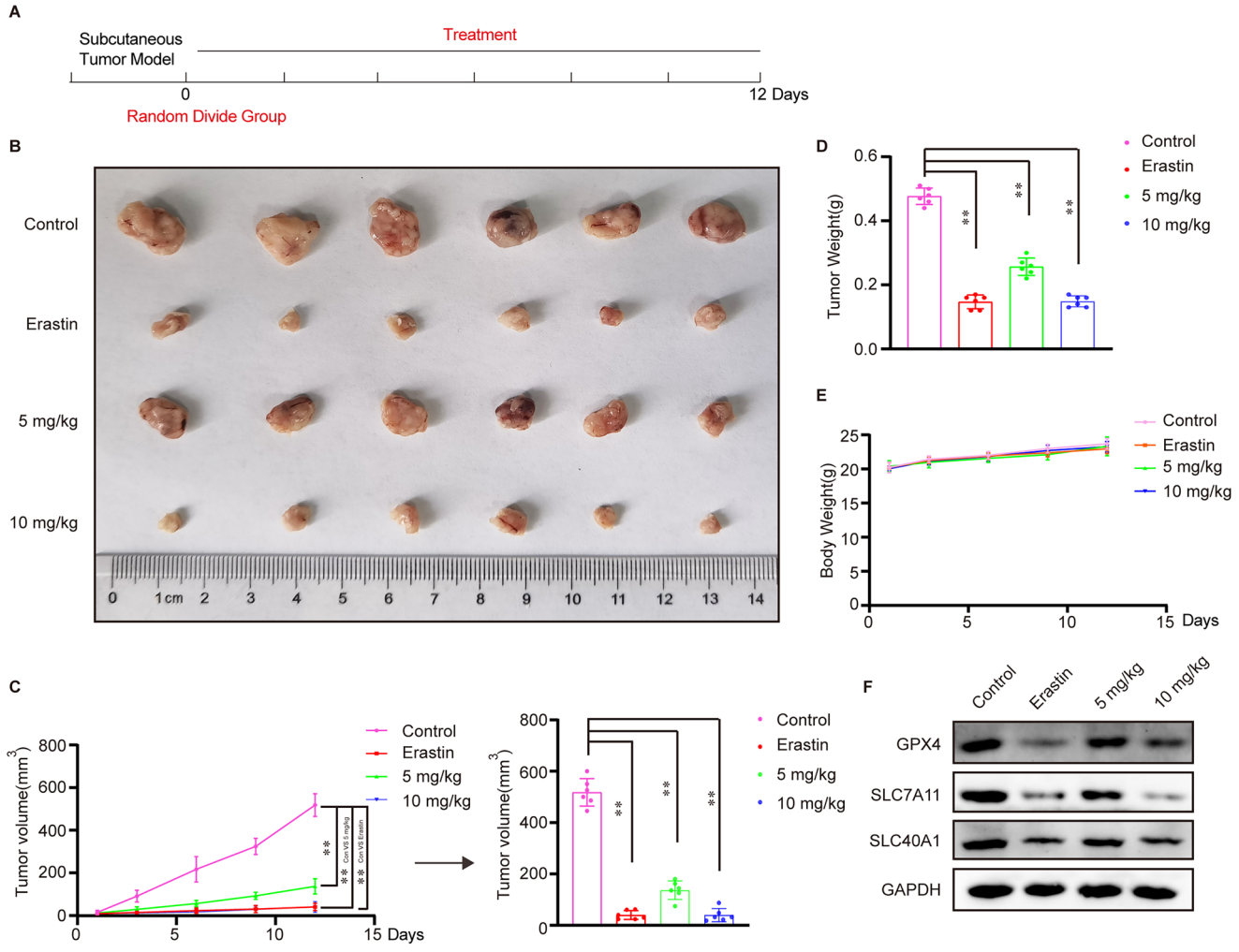

Figure 7. Inhibitory effect of cephaeline on lung cancer cells *in vivo*. (A) Schematic diagram of the anti-lung cancer effect of cephaeline *in vivo*. (B) The antitumour effect of erastin (20 mg/kg) and cephaeline (5 and 10 mg/kg) *in vivo* were studied by using the subcutaneous tumor xenograft model, $n = 6$. (C and D) The tumor volume and tumor weight were measured both in control group, erastin group and cephaeline treatment group, Mean ± SD, $^{**}p < 0.01$ *vs.* the control group. (E) The body weight was measured both in control group, erastin group and cephaeline treatment group, Mean ± SD. (F) The proteins GPX4, SLC7A11 and SLC40A1 associated with ferroptosis were detected in tumor tissues by Western blotting.

peroxidation. Therefore, cephaeline-induced ferroptosis ultimately results from the inhibition of the antioxidant system and the exacerbation of lipid peroxidation.

NRF2 is a critical transcription factor has the function of regulating iron homeostasis and redox balance in cells, which is strongly associated with ferroptosis (Kerins and Ooi 2018; Zhang et al. 2021). Moreover, there are studies showing that the expression of NRF2 in normal samples is lower than that in LUAD samples, especially in advanced LUAD stages (Wang et al. 2008). Due to the mutant of KEAP1, an inhibitor of NRF2, lead to the strong and persistent induction of NRF2 in cancer tissues (Hellyer et al. 2021; Scalera et al. 2022). Therefore, NRF2 should be regarded as a potential target for tumor therapy. In our study, we found that cephaeline could promote the downregulation of NRF2. Existing studies have shown that NRF2 affects redox homeostasis by regulating its downstream target genes GPX4 and SLC7A11 (Shin et al. 2018; Dong et al. 2020). However, NRF2 affects iron homeostasis by regulating its downstream iron regulation-related protein SLC40A1 (Harada et al. 2011; Wu et al. 2017). Therefore, with this in mind, we believe that cephaeline inhibits NRF2, leading to the downregulation of the downstream key antioxidant proteins GPX4 and SLC7A11, resulting in the inhibition of the antioxidant system. In addition, cephaeline promotes iron overload in cells by downregulating SLC40A1, a key protein that promotes iron efflux, and upregulating transferrin, a key protein that regulates iron influx. These events in combination lead to the induction of ferroptosis. Subsequently, the NRF2 agonist TBHQ was used to reverse the inhibitory effects of cephaeline on lung cancer cells. We found that the antitumour effects of cephaeline were reversed. Moreover, we also found that TBHQ could restore redox homeostasis altered by cephaeline, thereby reversing the occurrence of ferroptosis.

Finally, we used a subcutaneous tumor xenograft model to investigate the antitumor effects of cephaeline. Our findings indicate that cephaeline exhibits significant and highly efficient antitumor effects. Furthermore, to verify the antitumour mechanism of cephaeline by inducing ferroptosis *in vivo*, the expression of key ferroptosis-associated proteins was measured in different groups of tumor tissues by western blotting. These results were consistent with the *in vitro* findings, which further confirmed that cephaeline plays an antitumour role by inducing ferroptosis.

Conclusions

Our study has demonstrated that cephaeline has a significant inhibitory effect on lung cancer cells by inducing ferroptosis. In

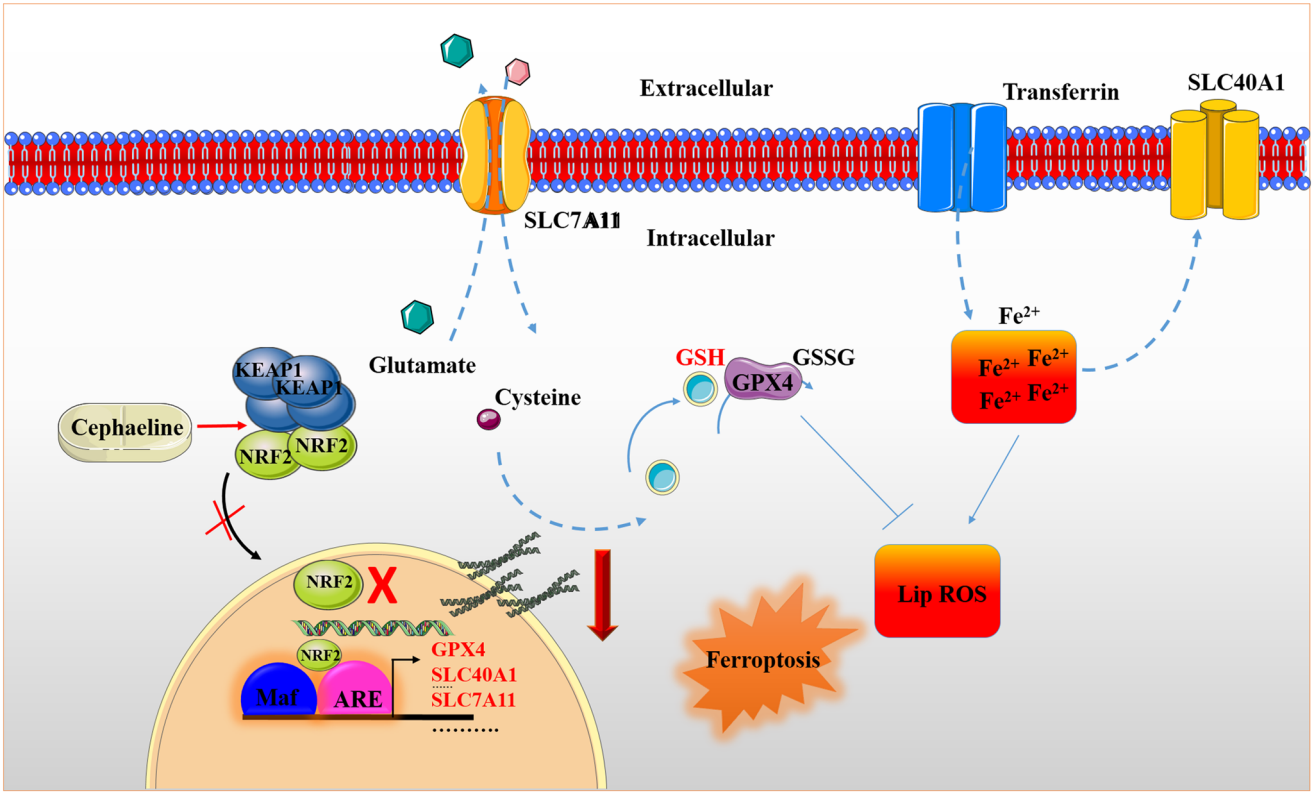

Figure 8. Schematic diagram of molecular mechanism of cephaeline's antitumour effect. Cephaeline inactivates NRF2 and reduces the expression of its downstream genes GPX4, SLC7A11 and SLC40A1. While the downregulation of *GPX4-SLC7A1* gene leads to the inhibition of antioxidant system, including the reduction of key antioxidant GSH. In addition, the downregulation of *SLC40A1* gene accompanied by upregulation of transferrin, resulting in a significant increase in intracellular iron ions. Finally, the level of lipid ROS increased and cell ferroptosis occurred.

addition, this study also demonstrated that NRF2 is a key target for cephaeline induced ferroptosis of lung cancer cells. The research on the anti-lung cancer efficacy of cephaeline and its mechanism will provide potential candidate drugs for the treatment of lung cancer patients in the clinic.

Author contributions

L.Z. and P. C. conceived the idea, analysed data, wrote the manuscript; Q. Y., S.L. and P. C. jointly performed the experiments.

Disclosure statement

The authors declare no competing interests.

Funding

This study was supported by National Natural Science Foundation of China (82204689) and Scientific Research Foundation of Hangzhou City University (Z2022066).

References

Akter R, Najda A, Rahman M, Shah M, Wesołowska S, Hassan S, Mubin S, Bibi P, Saeeda S. 2021. Potential role of natural products to combat radiotherapy and their future perspectives. Molecules. 28(24):5997. doi: 10.3390/molecules28248091.

Ashrafizadeh M, Najafi M, Makvandi P, Zarrabi A, Farkhondeh T, Samarghandian S. 2020. Versatile role of curcumin and its derivatives in lung cancer therapy. J Cell Physiol. 235(12):9241–9268. doi: 10.1002/jcp.29819.

Balaji S, Terrero D, Tiwari A, Ashby C, Raman D. 2021. Alternative approaches to overcome chemoresistance to apoptosis in cancer. Adv Protein Chem Struct Biol. 126:91–122. doi: 10.1016/bs.apcsb.2021.01.005.

Camidge D, Doebele R, Kerr K. 2019. Comparing and contrasting predictive biomarkers for immunotherapy and targeted therapy of NSCLC. Nat Rev Clin Oncol. 16(6):341–355. doi: 10.1038/s41571-019-0173-9.

Dierge E, Debock E, Guilbaud C, Corbet C, Mignolet E, Mignard L, Bastien E, Dessy C, Larondelle Y, Feron O. 2021. Peroxidation of n-3 and n-6 polyunsaturated fatty acids in the acidic tumor environment leads to ferroptosis-mediated anticancer effects. Cell Metab. 33(8):1701–1715.e1705. doi: 10.1016/j.cmet.2021.05.016.

Dixon S, Lemberg K, Lamprecht M, Skouta R, Zaitsev E, Gleason C, Patel D, Bauer A, Cantley A, Yang W, et al. 2012. Ferroptosis: an iron-dependent form of nonapoptotic cell death. Cell. 149(5):1060–1072. doi: 10.1016/j.cell.2012.03.042.

Dong H, Qiang Z, Chai D, Peng J, Xia Y, Hu R, Jiang H. 2020. Nrf2 inhibits ferroptosis and protects against acute lung injury due to intestinal ischemia reperfusion via regulating SLC7A11 and HO-1. Aging (Albany NY). 12(13):12943–12959. doi: 10.18632/aging.103378.

Gao M, Yi J, Zhu J, Minikes A, Monian P, Thompson C, Jiang X. 2019. Role of mitochondria in ferroptosis. Mol Cell. 73(2):354–363.e353. doi: 10.1016/j.molcel.2018.10.042.

Gao S, Li N, Wang S, Zhang F, Wei W, Li N, Bi N, Wang Z, He J. 2020. Lung cancer in People's Republic of China. J Thorac Oncol. 15(10):1567–1576. doi: 10.1016/j.jtho.2020.04.028.

Harada N, Kanayama M, Maruyama A, Yoshida A, Tazumi K, Hosoya T, Mimura J, Toki T, Maher J, Yamamoto M, et al. 2011. Nrf2 regulates ferroportin 1-mediated iron efflux and counteracts lipopolysaccharide-induced ferroportin 1 mRNA suppression in macrophages. Arch Biochem Biophys. 508(1):101–109. doi: 10.1016/j.abb.2011.02.001.

Hellyer J, Padda S, Diehn M, Wakelee H. 2021. Clinical implications of KEAP1-NFE2L2 mutations in NSCLC. J Thorac Oncol. 16(3):395–403. doi: 10.1016/j.jtho.2020.11.015.

Henning Y, Blind U, Larafa S, Matschke J, Fandrey J. 2022. Hypoxia aggravates ferroptosis in RPE cells by promoting the Fenton reaction. Cell Death Dis. 13(7):662. doi: 10.1038/s41419-022-05121-z.

Hirschhorn T, Stockwell B. 2019. The development of the concept of ferroptosis. Free Radic Biol Med. 133:130–143. doi: 10.1016/j.freeradbiomed.2018.09.043.

Huang Z, Jing X, Sheng Y, Zhang J, Hao Z, Wang Z, Ji L. 2019. (-)-Epicatechin attenuates hepatic sinusoidal obstruction syndrome by inhibiting liver oxidative and inflammatory injury. Redox Biol. 22:101117. doi: 10.1016/j.redox.2019.101117.

Kerins M, Ooi A. 2018. The roles of NRF2 in modulating cellular iron homeostasis. Antioxid Redox Signal. 29(17):1756–1773. doi: 10.1089/ars.2017.7176.

Liang J, Wang D, Lin H, Chen X, Yang H, Zheng Y, Li Y. 2020. A novel ferroptosis-related gene signature for overall survival prediction in patients with hepatocellular carcinoma. Int J Biol Sci. 16(13):2430–2441. doi: 10.7150/ijbs.45050.

Liu K, Ding L, Wu H. 2015. Bevacizumab in combination with anticancer drugs for previously treated advanced non-small cell lung cancer. Tumour Biol. 36(3):1323–1327. doi: 10.1007/s13277-014-2962-1.

Mao C, Liu X, Zhang Y, Lei G, Yan Y, Lee H, Koppula P, Wu S, Zhuang L, Fang B, et al. 2021. DHODH-mediated ferroptosis defence is a targetable vulnerability in cancer. Nature. 593(7860):586–590. doi: 10.1038/s41586-021-03539-7.

Qian L, Wang F, Lu S, Miao H, He X, Feng J, Huang H, Shi R, Zhang J. 2022. A comprehensive prognostic and immune analysis of ferroptosis-related genes identifies SLC7A11 as a novel prognostic biomarker in lung adenocarcinoma. J Immunol Res. 2022:1951620. doi: 10.1155/2022/1951620.

Qiang W, Dai Y, Xing X, Sun X. 2022. Identification of a metabolic reprogramming-related signature associated with prognosis and immune microenvironment of head and neck squamous cell carcinoma by *in silico* analysis. Cancer Med. 11(16):3168–3181. doi: 10.1002/cam4.4670.

Scalera S, Mazzotta M, Cortile C, Krasniqi E, De Maria R, Cappuzzo F, Ciliberto G, Maugeri-Saccà M. 2022. KEAP1-mutant NSCLC: the catastrophic failure of a cell-protecting Hub. J Thorac Oncol. 17(6):751–757. doi: 10.1016/j.jtho.2022.03.011.

Sha R, Xu Y, Yuan C, Sheng X, Wu Z, Peng J, Wang Y, Lin Y, Zhou L, Xu S, et al. 2021. Predictive and prognostic impact of ferroptosis-related genes ACSL4 and GPX4 on breast cancer treated with neoadjuvant chemotherapy. EbioMedicine. 71:103560. doi: 10.1016/j.ebiom.2021.103560.

Shin D, Kim E, Lee J, Roh J. 2018. Nrf2 inhibition reverses resistance to GPX4 inhibitor-induced ferroptosis in head and neck cancer. Free Radic Biol Med. 129:454–462. doi: 10.1016/j.freeradbiomed.2018.10.426.

Silva L, Borgato G, Wagner V, Martins M, Rocha G, Lopes M, Santos-Silva A, de Castro Júnior G, Kowalski L, Nor J, et al. 2022. Cephaeline is an inductor of histone H3 acetylation and inhibitor of mucoepidermoid carcinoma cancer stem cells. J Oral Pathol Med. 51(6):553–562. doi: 10.1111/jop.13252.

Sung H, Ferlay J, Siegel R, Laversanne M, Soerjomataram I, Jemal A, Bray F. 2021. Global cancer statistics 2020: GLOBOCAN estimates of incidence and mortality worldwide for 36 cancers in 185 countries. CA Cancer J Clin. 71(3):209–249. doi: 10.3322/caac.21660.

Wang D, Wei G, Ma J, Cheng S, Jia L, Song X, Zhang M, Ju M, Wang L, Zhao L, et al. 2021. Identification of the prognostic value of ferroptosis-related gene signature in breast cancer patients. BMC Cancer. 21(1):645. doi: 10.1186/s12885-021-08341-2.

Wang H, Liu C, Zhao Y, Gao G. 2020. Mitochondria regulation in ferroptosis. Eur J Cell Biol. 99(1):151058. doi: 10.1016/j.ejcb.2019.151058.

Wang X, Sun Z, Villeneuve N, Zhang S, Zhao F, Li Y, Chen W, Yi X, Zheng W, Wondrak G, et al. 2008. Nrf2 enhances resistance of cancer cells to chemotherapeutic drugs, the dark side of Nrf2. Carcinogenesis. 29(6):1235–1243. doi: 10.1093/carcin/bgn095.

Wu J, Bao L, Zhang Z, Yi X. 2017. Nrf2 induces cisplatin resistance via suppressing the iron export related gene SLC40A1 in ovarian cancer cells. Oncotarget. 8(55):93502–93515. doi: 10.18632/oncotarget.19548.

Xie Y, Hou W, Song X, Yu Y, Huang J, Sun X, Kang R, Tang D. 2016. Ferroptosis: process and function. Cell Death Differ. 23(3):369–379. doi: 10.1038/cdd.2015.158.

Yang Y, Bai L, Liao W, Feng M, Zhang M, Wu Q, Zhou K, Wen F, Lei W, Zhang N, et al. 2021. The role of non-apoptotic cell death in the treatment and drug-resistance of digestive tumors. Exp Cell Res. 405(2):112678. doi: 10.1016/j.yexcr.2021.112678.

Zhang L, Zhang J, Jin Y, Yao G, Zhao H, Qiao P, Wu S. 2021. Nrf2 is a potential modulator for orchestrating iron homeostasis and redox balance in cancer cells. Front Cell Dev Biol. 9:728172. doi: 10.3389/fcell.2021.728172.

Zhou B, Liu J, Kang R, Klionsky D, Kroemer G, Tang D. 2020. Ferroptosis is a type of autophagy-dependent cell death. Semin Cancer Biol. 66:89–100. doi: 10.1016/j.semcancer.2019.03.002.

Zhu G, Huang H, Xu S, Shi R, Gao Z, Lei X, Zhu S, Zhou N, Zu L, Mello R, et al. 2021. Prognostic value of ferroptosis-related genes in patients with lung adenocarcinoma. Thorac Cancer. 12(12):1890–1899. doi: 10.1111/1759-7714.13998.